



The AAPM/RSNA Physics Tutorial for Residents

Search for Isotropic Resolution in CT from Conventional through Multiple-Row Detector¹

Mahadevappa Mahesh, PhD

Computed tomography (CT) is a method of acquiring and reconstructing the image of a thin cross section on the basis of measurements of attenuation. In comparison with conventional radiographs, CT images are free of superimposing tissues and are capable of much higher contrast due to elimination of scatter. Most of the developments in CT since its introduction can be considered as attempts to provide faster acquisition times, better spatial resolution, and shorter computer reconstruction times. From the early designs, the technology progressed with faster scanning times and higher scanning plane resolution, but true three-dimensional (3D) imaging became practical only with helical scanning capabilities. The recent advent of multiple-row detector helical scanners has the capability to produce 3D images that approach the ideal of a true “3D radiograph.” Current multiple-row detector scanners can scan 40-cm volume lengths in less than 30 seconds with near-isotropic resolution and image quality that could not be envisioned at the time of Hounsfield’s invention.

©RSNA, 2002

Abbreviation: 3D = three-dimensional

Index terms: Computed tomography (CT) • Computed tomography (CT), helical • Computed tomography (CT), high-resolution • Computed tomography (CT), multi-detector row • Computed tomography (CT), physics • Computed tomography (CT), technology • Computed tomography (CT), thin-section • Computed tomography (CT), three-dimensional

RadioGraphics 2002; 22:949–962

¹From The Russell H. Morgan Department of Radiology and Radiological Sciences, Johns Hopkins University School of Medicine, 601 N Caroline St, Baltimore, MD 21287-0856. From the AAPM/RSNA Physics Tutorial at the 2001 RSNA scientific assembly. Received February 12, 2002; revision requested March 14 and received March 27; accepted April 16. **Address correspondence to** the author (e-mail: mmahesh@jhmi.edu).

©RSNA, 2002

Introduction

Since its introduction in 1972, x-ray computed tomography (CT) has evolved into an essential diagnostic imaging tool for a continually increasing variety of clinical applications. Dramatic improvements in image quality, acquisition speed, and patient throughput have resulted from recent technical developments in helical and, more recently, multiple-row detector technologies. This evolution of CT technology is a logical extension of conventional radiography and can be viewed as a progression toward optimizing the information content of radiographic images and extending the method to three dimensions.

In conventional x-ray imaging, a uniform x-ray beam is directed at the patient and exits the opposite surface encoded with intensity variations due to differential attenuation of x rays along different paths through the patient. The intensity-encoded pattern is then recorded on a two-dimensional surface (the radiographic image receptor). Radiographic systems have themselves evolved considerably, and current film-based systems promise spatial resolution in excess of 5 line pairs per millimeter (lp/mm) with acquisition times in the tens to hundreds of milliseconds. However, radiographic image quality has some limitations. Film-based systems are nonlinear, and the ability to discriminate small tissue differences is largely limited by poor scatter discrimination. One major problem that limits clinical usefulness is that radiographic images superimpose three-dimensional (3D) anatomy onto a two-dimensional surface. Historically, much of the training that radiologists have received has been dedicated to mentally reconstructing the 3D anatomic relationships from one or more radiographic projections with overlapping anatomy to determine whether altered patterns signal the presence of disease.

The ideal x-ray imaging system would combine the attributes of conventional radiography but also solve some of its limitations. Such a system would be able to produce images with spatial resolution on the order of 5 lp/mm and acquisition times of a few hundred milliseconds, sufficient to freeze physiologic motion. In addition, the ideal system would respond linearly over a wide range, exclude contrast-robbing scatter, and provide 3D information free of superimposing tissues with equal resolution throughout (isotropic resolution). Even the earliest CT scanners progressed toward this goal. Early scanners obtained images of transverse sections through the

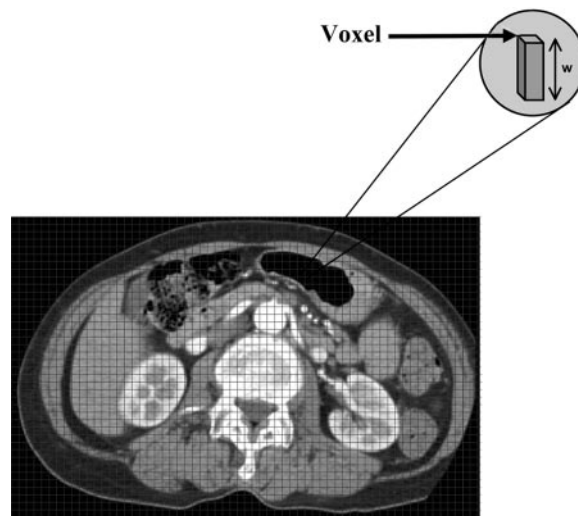


Figure 1. Sample CT image. A CT image is composed of *pixels* (picture elements). Each pixel on the image represents the average x-ray attenuation in a small volume (*voxel*) that extends through the tissue section. (In this example, the pixel size is exaggerated. In addition, in a real CT image, all tissues within a single pixel would be the same shade of gray.) w = width.

body, thus avoiding the problem of superimposed tissues. The narrow beam geometry and special collimation effectively eliminated scatter, thus greatly improving the contrast detectability over that of radiographic methods. With respect to spatial resolution and acquisition times, however, early scanners had a very long way to go to achieve near-radiographic performance in three dimensions.

The purpose of this article is to review the developmental path of CT technology from its beginnings to the multiple-row detector scanners of today in search of this “holy grail” of imaging, that is, the optimal 3D radiograph. Specific topics discussed are computed tomography, basic principles of CT, historical developments, CT generations, principles of helical CT scanners, capabilities of single-row detector helical CT, multiple-row detector helical CT, helical pitch, advantages of multiple-row detector CT, and future directions. This article is the first in a series of three on topics in CT and will be followed by articles on image reconstruction and processing and on radiation dose.

Computed Tomography

CT is fundamentally a method for acquiring and reconstructing an image of a thin cross section of an object (1–3). It differs from conventional projection in two significant ways: First, CT forms a cross-sectional image, eliminating the superimposition of structures that occurs in plane film imaging because of compression of 3D body structures

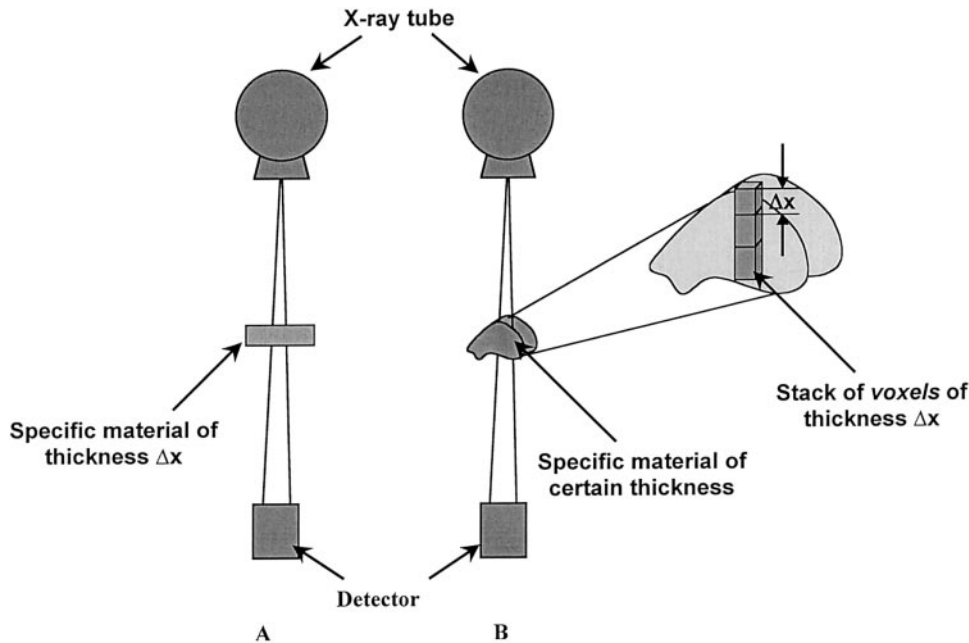


Figure 2. Principles of CT. Diagram shows the x-ray attenuation through a specific material of finite thickness (Δx) (Eq [1]) (A) and through a material considered as a stack of voxels with each voxel of finite thickness (Δx) (Eq [2]) (B).

onto the two-dimensional recording system. Second, the sensitivity of CT to subtle differences in x-ray attenuation is at least a factor of 10 higher than normally achieved by screen-film recording systems because of the virtual elimination of scatter (4).

Basic Principles of CT

Fundamentally, a CT scanner makes many measurements of attenuation through the plane of a finite-thickness cross section of the body. The system uses these data to reconstruct a digital image of the cross section, with each pixel in the image representing a measurement of the mean attenuation of a boxlike element (a voxel) that extends through the thickness of the section (Fig 1).

An attenuation measurement quantifies the fraction of radiation removed in passing through a given amount of a specific material of thickness Δx (Fig 2, A). Attenuation is expressed as follows:

$$I_t = I_0 e^{-\mu \Delta x}, \tag{1}$$

where I_t is the x-ray intensity measured with the material in the x-ray beam path, I_0 is the x-ray intensity measured without the material in the x-ray beam path, and μ is the linear attenuation coefficient of the specific material.

To illustrate CT principles, any material can be considered as a stack of voxels along the beam path (Fig 2, B). Each attenuation measurement is called a *ray sum* because attenuation along a spe-

cific straight-line path through the patient from the tube focal spot to a detector is the sum of the individual attenuations of all materials along the path. If it is assumed that the ray path through the tissue is broken up into incremental voxel thicknesses Δx , the transmitted intensity is given by the following formula:

$$I_t = I_0 e^{-\sum_{i=1}^k \mu_i \Delta x}, \tag{2}$$

where

$$-\sum_{i=1}^k \mu_i \Delta x = -(\mu_1 + \mu_2 + \mu_3 + \dots + \mu_k) \Delta x. \tag{3}$$

This formula is expressed as the natural logarithm (ln):

$$\ln\left(\frac{I_0}{I_t}\right) = \sum_{i=1}^k \mu_i \Delta x. \tag{4}$$

The image reconstruction process derives the average attenuation coefficient (μ) values for each voxel in the cross section by using many rays from many different rotational angles around the cross section. The specific attenuation of a voxel (μ)

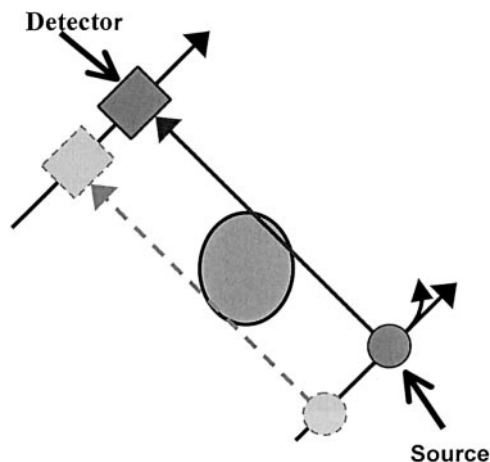


Figure 3. Diagram of the first-generation CT scanner, which used a parallel x-ray beam with translate-rotate motion to acquire data.

increases with the density and the atomic numbers of tissues averaged through the volume of the voxel and declines with increasing x-ray energy.

Mathematically, the attenuation value (μ) for each voxel could be determined algebraically with a very large number of simultaneous equations by using all ray sums that intersect the voxel. However, a much more elegant and simpler method called *filtered back-projection* was used in the early CT scanners and remains in use today (5). Rays are collected in sets called *projections*, which are made across the patient in a particular direction in the section plane. There may be from 500 to 1,000 or more rays in a single projection. To reconstruct the image from the ray measurements, each voxel must be viewed from multiple different directions. A complete data set requires many projections at rotational intervals of 1° or less around the cross section. Back-projection effectively reverses the attenuation process by adding the attenuation value of each ray in each projection back through the reconstruction matrix. Because this process generates a blurred image, the data from each projection are mathematically altered (filtered) prior to back-projection, eliminating the intrinsic blurring effect. There are a number of advanced reconstruction techniques that are currently used in the CT image reconstruction process; however, these are beyond the scope of this article (5–9).

As a final step, the individual voxel attenuation values are scaled to more convenient integers and

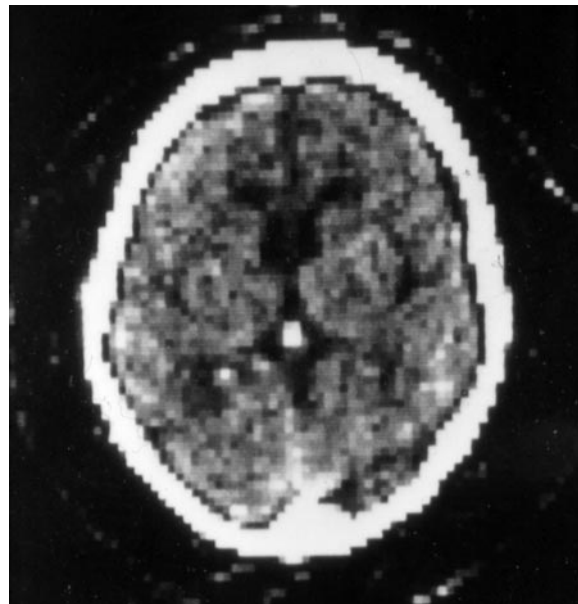


Figure 4. CT image of the head obtained with an early CT scanner. The scan plane resolution is on the order of 3 mm for a field of view of 25 cm with an 80×80 matrix and a z-axis resolution of approximately 13 mm.

normalized to voxel values containing water (μ_w). CT numbers are computed as follows:

$$\text{CT \#} = K \left(\frac{\mu_m - \mu_w}{\mu_w} \right), \quad (5)$$

where μ_m is the measured attenuation of the material in the voxel and K (1,000) is the scaling factor. The attenuation coefficient of water is obtained during calibration of the CT machine. Voxels containing materials that attenuate more than water (eg, muscle tissue, liver, and bone) have positive CT numbers, whereas materials with less attenuation than water (eg, lung or adipose tissues) have negative CT numbers. With the exception of water and air, the CT numbers for a given material will vary with changes in the x-ray tube potential and from manufacturer to manufacturer.

Historical Developments

In 1979, Sir Godfrey N. Hounsfield (10) and Alan M. Cormack were awarded the Nobel prize in medicine for the “development of computer assisted tomography.” The mathematical principles of image reconstruction date earlier to Radon in 1917. A variety of CT geometries have been developed to acquire the x-ray transmission

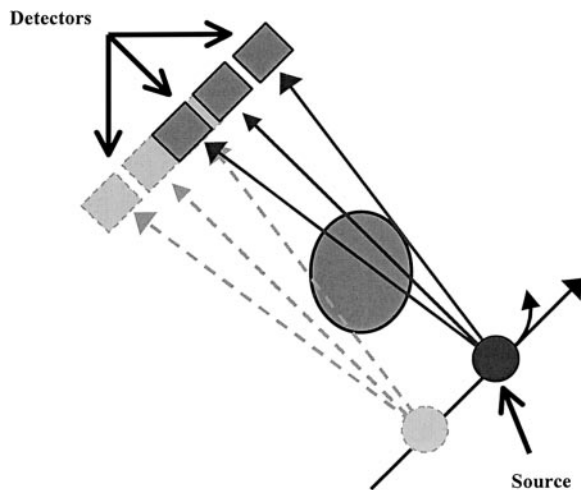


Figure 5. Diagram of the second-generation CT scanner, which used translate-rotate motion to acquire data.

data for image reconstruction. These geometries, commonly called *generations*, remain useful in differentiating scanner designs (1,2,6).

CT Generations

First-Generation CT Scanners

The EMI Mark I scanner, the first commercial scanner invented by Hounsfield, was introduced in 1973 (11). This scanner acquired data with an x-ray beam collimated to a narrow “pencil” beam directed to a single detector on the other side of the patient; the detector and the beam were aligned in a scanning frame. A single projection was acquired by moving the tube and detector in a straight-line motion (translation) on opposite sides of the patient (Fig 3). To acquire the next projection, the frame rotated 1° , then translated in the other direction. This process of translation and rotation was repeated until 180 projections were obtained. The earliest versions required about 4.5 minutes for a single scan and thus were restricted to regions where patient motion could be controlled (the head). Since procedures consisted of a series of scans, procedure time was reduced somewhat by using two detectors so that two parallel sections were acquired in one scan. Although the contrast resolution of internal structures was unprecedented, images had poor spatial

resolution (on the order of 3 mm for a field of view of 25 cm and 80×80 matrix) and very poor z-axis resolution (~ 13 -mm section thickness) (Fig 4).

Second-Generation CT Scanners

The main impetus for improvement was in reducing scan time ultimately to the point that regions in the trunk could be imaged. By adding detectors angularly displaced, several projections could be obtained in a single translation. For example, one early design used three detectors each displaced by 1° . Since each detector viewed the x-ray tube at a different angle, a single translation produced three projections. Hence, the system could rotate 3° to the next projection rather than 1° and had to make only 60 translations instead of 180 to acquire a complete section (Fig 5). Scan times were reduced by a factor of three. Designs of this type had up to 53 detectors, were ultimately fast enough (tens of seconds) to permit acquisition during a single breath hold, and thus were the first designs to permit scans of the trunk of the body. Because rotating anode tubes could not withstand the wear and tear of rotate-translate motion, this early design required a relatively low output stationary anode x-ray tube. The power limits of stationary anodes for efficient heat dissipation were improved somewhat with the use of asymmetrical focal spots (smaller in the scan plane than in the z-axis direction), but this resulted in higher radiation doses due to poor beam restriction to the scan plane. Nevertheless, these scanners required slower scan speeds to obtain adequate x-ray flux at the detectors when scanning thicker patients or body parts.

Third-Generation CT Scanners

Designers realized that if a pure rotational scanning motion could be used, then it would be possible to use higher-power, rotating anode x-ray tubes and thus improve scan speeds in thicker body parts. One of the first designs to do so was the so-called third generation or rotate-rotate geometry. In these scanners, the x-ray tube is collimated to a wide, fan-shaped x-ray beam and directed toward an arc-shaped row of detectors.



Figure 8. Reconstruction image of the femora shows the “step-contour” nature of early 3D images. The image was produced by stacking two-dimensional cross-sectional CT images obtained with a conventional CT scanner.

cable unwinding, which resulted in longer examination times. The z-axis resolution was limited by the choice of section thickness, which ranged from 1 to 10 mm. For thicker sections, the partial volume averaging between different tissues led to partial volume artifacts. These artifacts were reduced to some extent by scanning thinner sections. In addition, even though it was possible to obtain 3D images by stacking thin sections, inaccuracy dominated due to involuntary motion from scan to scan. A typical 3D reconstruction of this era is shown in Figure 8. The steplike contours could be minimized by overlapping of CT sections at the expense of a significant increase in radiation to the patient. Also, the conventional method of section-by-section acquisition produced misregistration of lesions between sections due to involuntary motion of anatomy in subsequent breath holds between scans. It was soon realized that if multiple sections could be acquired in a single breath hold, a considerable improvement in the ability to image structures in regions susceptible to physiologic motion could

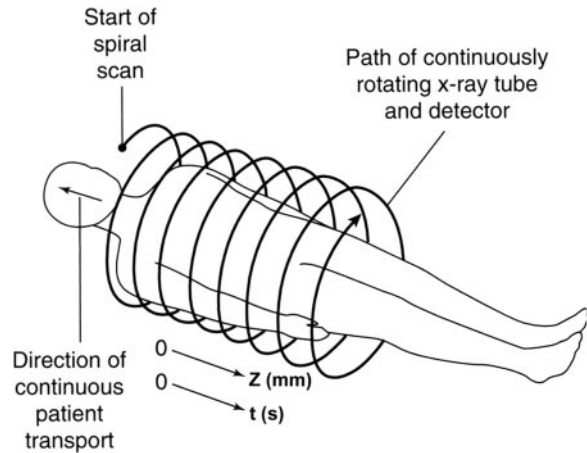


Figure 9. Principles of helical CT. As the patient is transported through the gantry, the x-ray tube traces a spiral or helical path around the patient, acquiring data as it rotates. t = time in seconds.

result. However, this required some technological advances, which led to the development of helical CT scanners.

Principles of Helical CT Scanners

The development of helical or spiral CT around 1990 was a truly revolutionary advancement in CT scanning that finally allowed true 3D image acquisition within a single breath hold. The technique involves the continuous acquisition of projection data through a 3D volume of tissue by continuous rotation of the x-ray tube and detectors and simultaneous translation of the patient through the gantry opening (Fig 9) (12). Three technological developments were required: slipping gantry designs, very high power x-ray tubes, and interpolation algorithms to handle the non-coplanar projection data (13).

Slip-Ring Technology

Slip rings are electromechanical devices consisting of circular electrical conductive rings and brushes that transmit electrical energy across a moving interface. All power and control signals from the stationary parts of the scanner system are communicated to the rotating frame through the slip ring. The slip-ring design consists of sets of parallel conductive rings concentric to the gantry axis that connect to the tube, detectors, and

control circuits by sliding contactors (Fig 10). These sliding contactors allow the scan frame to rotate continuously with no need to stop between rotations to rewind system cables (14). This engineering advancement resulted initially from a desire to reduce interscan delay and improve throughput. However, reduced interscan delay increased the thermal demands on the x-ray tube; hence, tubes with much higher thermal capacities were required to withstand continuous operation over multiple rotations.

High-Power X-ray Tubes

X-ray tubes are subjected to far higher thermal loads in CT than in any other diagnostic x-ray application. In early CT scanners, such as in first- and second-generation, stationary anode x-ray tubes were used, since the long scan times meant that the instantaneous power level was low. Long scan times also allowed heat dissipation. Shorter scan times in later versions of CT scanners required high-power x-ray tubes and use of oil-cooled rotating anodes for efficient thermal dissipation. Heat storage capacities varied from 1 million to 3 million heat units in early third-generation CT scanners. The introduction of helical CT with continuous scanner rotation placed new demands on x-ray tubes.

Several technical advances in component design have been made to achieve these power levels and deal with the problems of target temperature, heat storage, and heat dissipation. For example, the tube envelope, cathode assembly, and anode assemblies including anode rotation and target design have been redesigned (15). As scan times have decreased, anode heat capacities have increased by as much as a factor of five, preventing the need for cooling delays during most clinical procedures, and tubes with capacities of 5–8 million heat units are available. In addition, improvement in the heat dissipation rate (kilo-heat units per minute) has increased the heat storage capacity of modern x-ray tubes. The large heat capacities are achieved with thick graphite backing of target disks, anode diameters of 200 mm or more, improved high-temperature rotor bearings, and metal housings with ceramic insulators (Fig 11), among other factors. The working life of tubes used to date ranges from 10,000 to 40,000 hours, compared with the 1,000 hours typical of conventional CT tubes. Because many of the engineering changes increased the mass of the tube, much of the design effort was also dedicated to reducing the mass to better withstand increasing gantry rotational rates required by ever faster scan times.

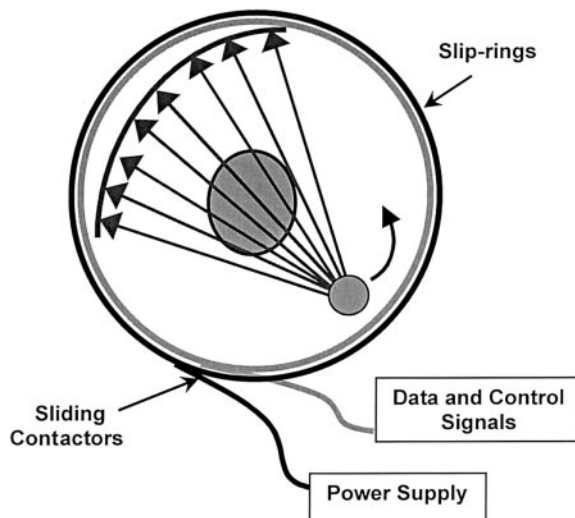


Figure 10. Diagram of the slip-ring configuration. Sliding contactors permit continuous rotation of the x-ray tube and detectors while maintaining electrical contact with stationary components.

Interpolation Algorithms

Conventional scanners stepped the patient through the gantry to provide a series of contiguous sections, but it was soon realized that if acquisition could be done with continuous table motion a much more satisfactory result would be obtained. The problem with continuous tube and table motion was that projections precessed in a helical motion around the patient and did not lie in a single plane. This meant that conventional reconstruction algorithms could not work.

Willi Kalender (12,16) is credited with solving this problem by developing interpolation methods to generate projections in a single plane so that conventional back-projections could be employed. There were several important benefits to this development. First, the reconstruction planes could be placed in any arbitrary position along the scanned volume encompassed by the table traverse during multiple rotations. This meant that sections could be overlapping along the scan axis, thus greatly improving data sampling and making 3D reconstructions practical. Second, since images can be acquired in a single breath hold, the 3D reconstructions are free of the misregistration artifacts caused by involuntary motion that limit conventional CT. True 3D volumes could be acquired that can be viewed in any perspective, making the promise of true 3D radiography a practical reality. A final benefit was that since overlapping sections were generated by mathematical methods rather than overlapping x-ray beams, the improved z-axis sampling was achieved without a radiation dose penalty to the patient. A number of advanced interpolation al-

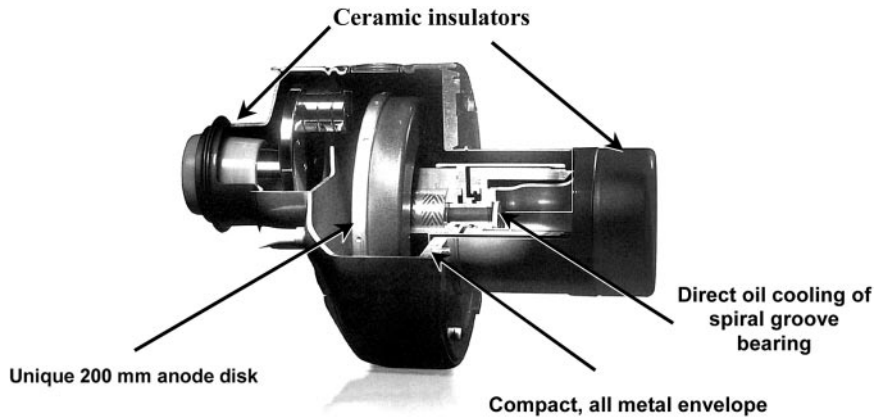


Figure 11. Photograph of a rotating anode x-ray tube used in helical CT scanners. Modern x-ray tubes have a capacity of 5–8 million heat units and contain large anode disks with ceramic insulators. (Courtesy of Philips Medical Systems, Shelton, Conn.)



Figure 12. Three-dimensional image reconstructed from single-row detector helical CT data. (Courtesy of Elliot Fishman, MD, Johns Hopkins Hospital, Baltimore, Md.)

gorithms were developed, with differing effects on image quality, but these are beyond the scope of this article (5,7).

During helical scans, the table motion causes displacement of the fan beam projections along the z axis; the relative displacement is a function of the table speed and the beam width. The ratio of table displacement per 360° rotation to section thickness is termed *pitch*, an important dimensionless quantity with implications for patient dose and image quality. For example, a pitch less

than 1 implies overlapping of anatomy and hence higher patient dose, whereas a pitch greater than 1 implies extended imaging and lower patient dose. Pitch values in clinical practice with these scanners typically range from 1 to 2.

Capabilities of Single-Row Detector Helical CT

With the advent of helical CT, considerable progress was made on the road toward 3D radiography. An example of a 3D reconstruction from single-row detector helical scanning is shown in Figure 12. Complete organs could be scanned in about 30–40 seconds; artifacts due to patient motion and tissue misregistration due to involuntary motion were virtually eliminated. It became possible to generate sections in any arbitrary plane through the scanned volume (17,18). Significant improvements in z-axis resolution were achieved due to improved sampling, since sections could be reconstructed at fine intervals less than the section width along the z axis. Near-isotropic resolution could be obtained with the thinnest (~1 mm) section widths at a pitch of 1, but this could be done only over relatively short lengths due to tube and breath-hold limitations (19,20). Higher-power tubes capable of longer continuous operation coupled with faster rotation speeds could scan greater lengths with higher resolution. The practical limit on such brute force approaches, however, became the length of time a sick patient could reliably suspend breathing. This turns out to be no more than 30 seconds. Even though the z-axis resolution for helical CT images far exceeds that of conventional CT images, the type of interpolation algorithm and the pitch still affect the overall image quality. The

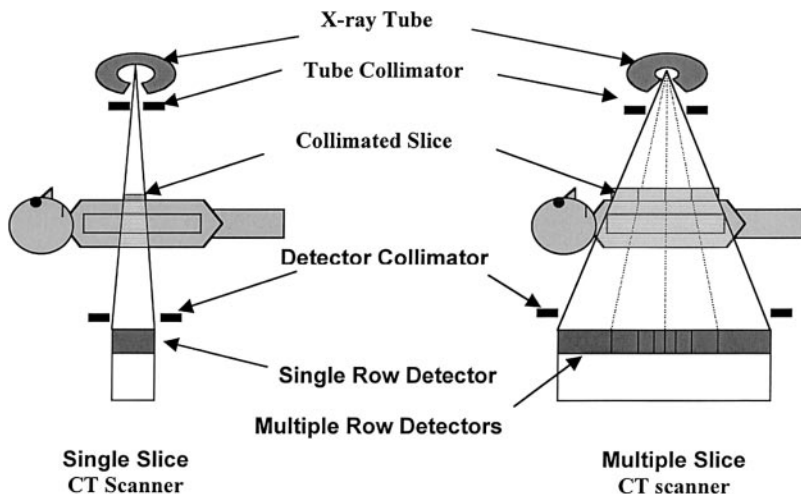


Figure 13. Diagram shows the difference between single-row detector and multiple-row detector CT designs. The multiple-row detector array shown is asymmetrical and represents that of one particular manufacturer.

section sensitivity profiles of helical CT images are different compared with those of conventional CT images, which are influenced by the type of interpolation algorithm and the selected pitch.

Multiple-Row Detector Helical CT

Continued scanner development on the road to a 3D radiograph called for further progress, but single-row detector helical scanners had reached their limits. An obvious improvement would be to make more efficient use of the x rays that are produced by the tube while improving z-axis spatial resolution; this led to the development of multiple-row detector arrays. The principal difference between single- and multiple-row detector helical scanners is illustrated in Figure 13. The basic idea actually dates to the very first EMI Mark I scanner, which had two parallel detectors and acquired two sections simultaneously. The first helical scanner to use this idea, the CT Twin (Elscent, Haifa, Israel), was launched in 1992. This design was so superior to single-row detector designs that all scanner manufacturers went back to the drawing board. By late 1998, all major CT manufacturers launched multiple-row detector CT scanners capable of acquiring at least four sections per rotation. The arrangement of detectors along the z axis and the widths of the available sections vary between the systems. Figure 14 illustrates different multiple-row detector array configurations from several manufacturers. The

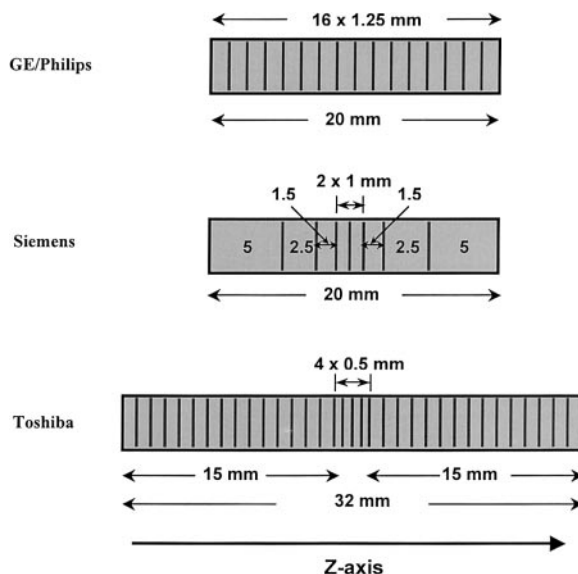


Figure 14. Various detector array designs used in multiple-row detector CT scanners.

possible combinations of section widths available for each configuration are listed in Table 1.

In single-row detector helical CT designs, scan volume can be increased with an increased pitch at the expense of poorer z-axis resolution, whereas z-axis resolution can be preserved in multiple-row detector designs. For example, if a 10-mm collimation were divided into four 2.5-mm detectors, the same scan length could be obtained in the same time but with a z-axis resolution improved from 10 mm to 2.5 mm. In an-

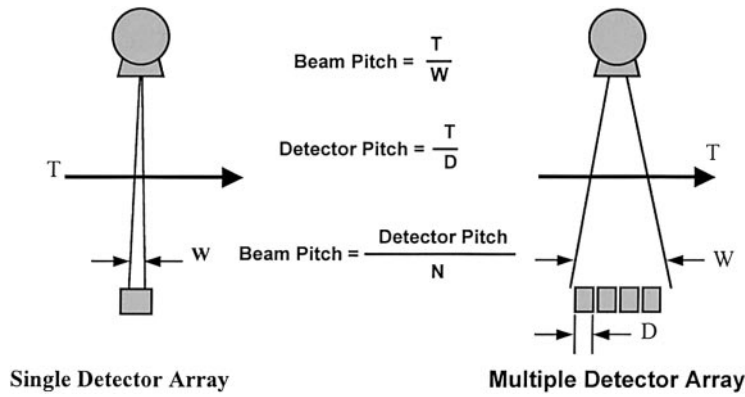


Figure 15. Diagram shows the concepts of beam pitch and detector pitch. Beam pitch is consistent with the previous notion of pitch used in single-row detector helical CT and works well for multiple-row detector CT scanners as well (22). D = detector width, N = number of active detectors, T = table travel per gantry rotation, W = beam width.

Table 1
Available Section Width Combinations
for Different Multiple-Row Detector
CT Configurations

GE*/Philips	Siemens†	Toshiba‡
4 × 1.25	2 × 0.5	4 × 0.5
4 × 2.5	4 × 1	4 × 1
4 × 3.75	4 × 2.5	4 × 2
4 × 5	4 × 5	4 × 3
2 × 10	2 × 8	4 × 4
	2 × 10	4 × 5
		4 × 6
		4 × 7
		4 × 8

Note.—Values are number of sections times section width (millimeters).
 *GE Medical Systems, Milwaukee, Wis.
 †Siemens Medical Systems, Iselin, NJ.
 ‡Toshiba Medical Systems, Tustin, Calif.

other example, a multiple-row detector scanner with four 5-mm detectors and a beam width of 20 mm reduces the scan time by a factor of 4–15 seconds for the same z-axis resolution (21). By increasing the number of CT scanner detector rows, data acquisition capability dramatically increases while greatly improving the efficiency of x-ray tubes. Further developments in scanner rotational speeds and tube outputs have made isotropic resolution a practical possibility with even better improvements on the horizon. Current multiple-row detector scanners can scan large 40-cm volume lengths in less than 30 seconds with near-isotropic resolution and image quality that could not be envisioned at the time of Hounsfield’s invention.

Helical Pitch

With single-row detector helical CT scanners, the concept of pitch is straightforward. With the beam width given by W (in millimeters) and the table travel per gantry rotation defined as T (in millimeters), pitch and more specifically the *beam pitch* (22) is defined as follows (Fig 15):

$$\text{Beam Pitch} = \frac{T}{W}. \tag{6}$$

With the introduction of multiple-row detector CT scanners, ambiguity arises in terms of the definition of pitch, since different manufacturers use different definitions of pitch (23), which has resulted in much confusion (24). Consequently, beam pitch needs to be distinguished from *detector pitch*, which is defined as follows:

$$\text{Detector Pitch} = \frac{T}{D}, \tag{7}$$

where D is the detector width in millimeters (Fig 15). If the x-ray beam is collimated to N active detectors in a multiple-row detector CT scanner, the relationship between beam pitch and collimator pitch is as follows:

$$\text{Beam Pitch} = \frac{\text{Detector Pitch}}{N}. \tag{8}$$

The use of beam pitch is applicable equally to both single-row detector helical CT and multiple-row detector CT and eliminates the confusion existing between the relationship of radiation dose and various manufacturers’ defined pitch (25).

Table 2
Comparison of Scanning Time between Single-Row Detector and Multiple-Row Detector CT Scanners

Region Scanned	Distance (cm)	Section Thickness (mm)	Scanning Time (sec) by Scanner	
			Single-Row Detector*	Multiple-Row Detector†
Head	20	8	16.7	2.1
Neck	15	5	20.0	2.5
Chest	30	8	25.0	3.1
Abdomen	20	8	16.7	2.1
Pelvis	20	8	16.7	2.1
All regions	105	...	95.1	11.9

*Scanner with 1-second rotation and a pitch of 1.5.

†Scanner with 0.5-second rotation and a pitch equivalent to 1.5.

Advantages of Multiple-Row Detector CT

The clinical advantages of multiple-row detector technology can be broadly divided into two categories: (a) Its speed can be used for fast imaging of large volumes of tissue with wide sections. This is particularly useful in studies where patient motion is a limiting factor. With a four-section system and a 0.5-second rotation, the volume data can be acquired eight times faster than with a single-row detector, 1-second scanner (Table 2). (b) The other main advantage of multiple-row detector systems is their ability to cover large volumes in short scan times. The volume coverage and speed performance in a multiple-row detector CT scanner are better than in its counterpart single-row detector helical CT scanner without compromises in image quality.

One of the most important promises of multiple-row detector technology is that of true isotropic spatial resolution, that is, cubic voxels, so that the image is equally sharp in any plane traversing the scanned volume. This capability is reasonably achieved with multiple sections of 1-mm thickness or less. Ideally, the true 3D radiograph would have cubic voxels of less than 1 mm acquired over large volumes with very short times, at least within a reasonable breath hold. CT angiography, which was possible with the single-row detector helical scanners, became practical with multiple-row detector scanners.

The fast rotation times and large volume coverage provide improved multiplanar reconstruction and 3D images (26,27) with reduced image artifacts (Fig 16). This technology also opens up new possibilities for applications in trauma, geriatric, and pediatric examinations. Improved accuracy in 3D volume coverage has led to the development of CT fluoroscopy and CT virtual endoscopy.

Future Directions

CT technology has evolved considerably over the past 30 years (Fig 17). With the development of multiple-row detector CT, clinical scanners capable of producing eight to 32 sections per second are available. The next logical step is to increase the number of detector arrays; however, the problem of cone beam artifacts becomes significant with the current reconstruction methods. Future developments in the directions of cone beam reconstructions are under way, and the next-generation CT scanners will adopt this method so that large area detectors can replace multiple-array detectors. Area detectors such as the flat panel detectors currently introduced in general radiography will find applications in CT. With substantial z-axis coverage, it will be possible to scan most organs in one or two rotations. Scan times may be further reduced to 150 msec as the gantry is redesigned to withstand very high centrifugal force. The days of single rotation of the gantry resulting in coverage of almost the entire body are not too distant. This can lead to far-reaching applications such as comprehensive screening examinations. Image reconstruction times will continue to decrease, partly from the



Figure 16. Three-dimensional image reconstructed from multiple-row detector helical CT data. (Courtesy of Elliot Fishman, MD.)

pressure of vast numbers of images that will be generated by CT examinations. With increased awareness about the radiation dose encountered during CT scanning, developments are under way to develop real-time exposure control to reduce radiation dose without loss of image quality by measuring attenuation within the patient during scanography or scout scanning and thereby adjusting the tube current during each gantry rotation.

Conclusions

Early CT scanners required long scan times and produced poor-resolution images. However, when compared with conventional radiographs, the images were free of superimposing tissues and exhibited high contrast due to elimination of scatter. CT technology has continued to evolve with improved resolution and scan time. With today's multiple-row detector helical CT scanners, 3D images can be obtained with spatial resolution approaching that of conventional radiographic images in all three dimensions.

Acknowledgment: The author thanks Thomas J. Beck, ScD, for useful discussions during preparation of the manuscript and the presentation at the 2001 AAPM/RSNA Physics Tutorial for Residents.

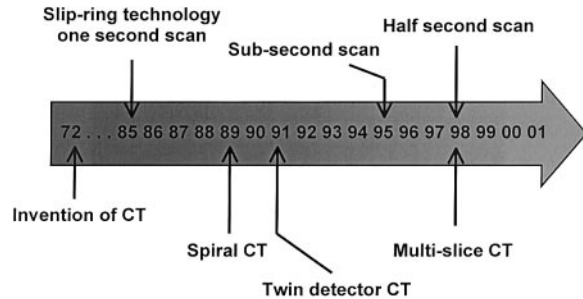


Figure 17. Time line of the key technological developments in CT.

References

1. Hendee WR, Ritenour R. Medical imaging physics. St Louis, Mo: Mosby, 1992.
2. Bushberg JT, Siebert JA, Leidholdt EM, Boone JM. The essential physics of medical imaging. Baltimore, Md: Williams & Wilkins, 1993.
3. Zatz L. General overview of computed tomography instrumentation. In: Potts D, ed. Radiology of the skull and brain: technical aspects of computed tomography. St Louis, Mo: Mosby, 1981; 4025–4057.
4. Gould RG. CT overview and basics. In: Gould RG, ed. Specification, acceptance testing and quality control of diagnostic x-ray imaging equipment. AAPM Monograph 20. New York, NY: American Institute of Physics, 1994; 801–831.
5. Napel S. Computed tomography image reconstruction. In: Fowlkes JB, ed. Medical CT and ultrasound: current technology and applications. Madison, Wis: Advanced Medical Publishing, 1995; 311–327.
6. Seeram E. Computed tomography: physical principles, clinical applications, and quality control. Philadelphia, Pa: Saunders, 2001.
7. Hsieh J. A general approach to the reconstruction of x-ray helical computed tomography. *Med Phys* 1996; 23:221–229.
8. Hu H. Multi-slice helical CT: scan and reconstruction. *Med Phys* 1999; 26:5–18.
9. Taguchi K, Aradate H. Algorithm for image reconstruction in multi-slice helical CT. *Med Phys* 1998; 25:550–561.
10. Hounsfield GN. Nobel Award address: computed medical imaging. *Med Phys* 1980; 7:283–290.
11. Hounsfield GN. Computerized transverse axial scanning (tomography). I. Description of system: 1973. *Br J Radiol* 1995; 68:H166–H172.
12. Kalender WA, Seissler W, Klotz E, Vock P. Spiral volumetric CT with single-breath-hold technique, continuous transport, and continuous scanner rotation. *Radiology* 1990; 176:181–183.

13. Beck TJ. CT technology overview: state of the art and future directions. In: Gould RG, Boone JM, eds. *Syllabus: a categorical course in physics—technology update and quality improvement of diagnostic x-ray imaging equipment*. Oak Brook, Ill: Radiological Society of North America, 1996; 161–172.
14. Brunnett CJ, Heuscher DJ, Mattson RA, Vrettos CJ. CT design considerations and specifications. In: Gould RG, ed. *Specification, acceptance testing and quality control of diagnostic x-ray imaging equipment*. AAPM Monograph 20. New York, NY: American Institute of Physics, 1994; 833–861.
15. Fox SH. CT tube technology. In: Fowlkes JB, ed. *Medical CT and ultrasound: current technology and applications*. Madison, Wis: Advanced Medical Publishing, 1995; 349–377.
16. Kalender WA, Polacin A. Physical performance characteristics of spiral CT scanning. *Med Phys* 1991; 18:910–915.
17. Fishman EK, Magid D, Ney DR, et al. Three-dimensional imaging. *Radiology* 1991; 181:321–337.
18. Zeman RK, Baron RL, Jeffrey RB Jr, Klein J, Siegel MJ, Silverman PM. Helical body CT: evolution of scanning protocols. *AJR Am J Roentgenol* 1998; 170:1427–1438.
19. Kalender WA. Thin-section three-dimensional spiral CT: is isotropic imaging possible? *Radiology* 1995; 197:578–580.
20. Levy RA. Three-dimensional craniocervical helical CT: is isotropic imaging possible? *Radiology* 1995; 197:645–648.
21. Hu H, He HD, Foley WD, Fox SH. Four multi-detector-row helical CT: image quality and volume coverage speed. *Radiology* 2000; 215:55–62.
22. Boone JM. Computed tomography: technology update on multiple detector array scanners and PACS considerations. In: Andriole KP, ed. *Practical digital imaging and PACS*. AAPM Monograph 25. Madison, Wis: Medical Physics Publishing, 1994; 37–63.
23. *IMPACT technology update: multi-slice CT scanners*. London, England: IMPACT, 1999.
24. Silverman PM, Kalender WA, Hazle JD. Common terminology for single and multislice helical CT. *AJR Am J Roentgenol* 2001; 176:1135–1136.
25. Mahesh M, Scatarige JC, Cooper J, Fishman EK. Dose and pitch relationship for a particular multi-slice CT scanner. *AJR Am J Roentgenol* 2001; 177:1273–1275.
26. Lawler LP, Fishman EK. Multi-detector row CT of thoracic disease with emphasis on 3D volume rendering and CT angiography. *RadioGraphics* 2001; 21:1257–1273.
27. Fishman EK, Kuszyk B. 3D imaging: musculoskeletal applications. *Crit Rev Diagn Imaging* 2001; 42:59–100.